TECHNICAL REPORT STANDARD PAGE

1. Title and Subtitle
   Development of Durable Self-Sensing Cementitious Composites (SSC) for Transportation Infrastructures Rehabilitation and Monitoring
2. Author(s)
   Khalilullah Taj; Yen-Fang Su
3. Performing Organization Name and Address
   Department of Civil & Environmental Engineering,
   Louisiana State University
   3255 Patrick F. Taylor Hall
   Baton Rouge, LA, 70803
4. Sponsoring Agency Name and Address
   Louisiana Department of Transportation and Development
   P.O. Box 94245
   Baton Rouge, LA 70804-9245
5. Report No.
   FHWA/LA.24/24-4TIRE
6. Report Date
   July 2024
7. Performing Organization Code
   LTRC Project Number: 24-4TIRE
   SIO Number: DOTLT1000499
8. Type of Report and Period Covered
   Final Report
   July 2023- June 2024
9. No. of Pages
   47
10. Supplementary Notes
    Conducted in Cooperation with the U.S. Department of Transportation, Federal Highway Administration
11. Distribution Statement
    Unrestricted. This document is available through the National Technical Information Service, Springfield, VA 21161.
12. Key Words
    Self-sensing concrete, piezoresistivity, structural health monitoring
13. Abstract

Self-sensing cementitious composites (SSC) are novel multifunctional infrastructure materials with excellent mechanical properties. Most importantly, they enable intrinsic sensory functionality within the structure. Thus, SSC has the potential to be a great alternative to conventional concrete for designing next-generation sustainable and resilient transportation infrastructure.

The underlying mechanism of the self-sensing behavior is through the piezoresistivity effect, which is facilitated by electrically conductive filler in cementitious materials. The changes in the internal structures of concrete can be captured by measuring the resistivity of materials, enabling civil engineers to gauge real-time strain-stress conditions. However, the effect of conductive fillers in the concrete that allows for the limited transfer of electrical charges on the durability properties, including corrosion resistance of rebars in concrete and chloride penetration, is still obscure.

In this study, different types and varying dosages of conductive fibers were designed in cementitious mortar to achieve the ideal sensitivity. The fractional change in resistivity and gauge factor were determined under cyclic and monotonic loading on top of quantifying the 1, 3, 7, and 28-day compressive strength. Subsequently, durability tests such as rapid chloride penetration and half-cell potential corrosion on the elected mixtures were performed. The results of this study reveal that a remarkable gauge factor of ~40 was achieved in the mix containing 0.5 wt% carbon fiber, which paralleled the efficiency of graphene oxide. Moreover, based on observations from the rapid chloride penetration test, the addition of carbon fiber in concrete decreased the risk of chloride ingress in harsh environments. Results from the half-cell potential corrosion test indicate that the designed SSC presents a fairly low risk of rebar corrosion in concrete.

Project Review Committee

Each research project will have an advisory committee appointed by the LTRC Director. The Project Review Committee is responsible for assisting the LTRC Administrator or Manager in the development of acceptable research problem statements, requests for proposals, review of research proposals, oversight of approved research projects, and implementation of findings.

LTRC appreciates the dedication of the following Project Review Committee Members in guiding this research study to fruition.

LTRC Administrator/Manager

Vijaya Gopu, Ph.D., P.E.

Directorate Implementation Sponsor

Chad Winchester, P.E.

DOTD Chief Engineer

Development of Durable Self-Sensing Cementitious Composites (SSC) for Transportation Infrastructures Rehabilitation and Monitoring

By
Khalilullah Taj, Graduate Research Assistant
Yen-Fang Su, Assistant Professor

Department of Civil and Environment Engineering
Louisiana State University and A&M College
3255 Patrick F. Taylor Hall, Baton Rouge, LA 70803

LTRC Project No. 24-4 TIRE
SIO No. DOTLT1000499

conducted for
Louisiana Department of Transportation and Development
Louisiana Transportation Research Center

July 2024

Abstract

Self-sensing cementitious composites (SSC) are novel multifunctional infrastructure materials with excellent mechanical properties; most importantly, they enable intrinsic sensory functionality within the structure. Thus, SSC has the potential to be a great alternative to conventional concrete for designing next-generation sustainable and resilient transportation infrastructure.

The underlying mechanism of the self-sensing behavior is through the piezoresistivity effect, which is facilitated by electrically conductive filler in cementitious materials. The changes in the internal structures of concrete can be captured by measuring the resistivity of materials, enabling civil engineers to gauge real-time strain-stress conditions. However, the effect of conductive fillers in the concrete that allows for the limited transfer of electrical charges on the durability properties, including corrosion resistance of rebars in concrete and chloride penetration, is still obscure.

In this study, different types and varying dosages of conductive fibers were designed in cementitious mortar to achieve the ideal sensitivity. The fractional change in resistivity and gauge factor were determined under cyclic and monotonic loading on top of quantifying the 1, 3, 7, and 28-day compressive strength. Subsequently, durability tests such as rapid chloride penetration and half-cell potential corrosion on the elected mixtures were performed. The results of this study reveal that a remarkable gauge factor of ~40 was achieved in the mix containing 0.5 wt% carbon fiber, which paralleled the efficiency of graphene oxide. Moreover, based on observations from the rapid chloride penetration test, the addition of carbon fiber in concrete decreased the risk of chloride ingress in harsh environments. Results from the half-cell potential corrosion test indicate that the designed SSC presents a fairly low risk of rebar corrosion in concrete.

Acknowledgements

The investigators appreciate the Louisiana Transportation Research Center (LTRC) funding this project through the Transportation Innovation for Research Exploration (TIRE) Program. The authors would like to acknowledge the technical support provided by LTRC’s Concrete Research Manager, Dr. Zhen Liu, and Materials Research Administrator, Dr. Samuel B. Cooper III, and the administrative direction provided by Dr. Vijaya Gopu, LTRC's Associate Director.

Implementation Statement

The self-sensing cementitious composites developed in this study exhibit excellent mechanical properties, durability, and sensing performance. They have the potential to be implemented partially or entirely in various sections of transportation infrastructure, such as reinforced concrete columns, beams, slabs, and even pavements, to monitor structural integrity while strengthening the structures.

Table of Contents

List of Tables

List of Figures

Introduction

The deterioration of civil infrastructure is inevitable. Transportation infrastructure such as bridges, roads, and so on will age and deteriorate due to material degradation, environmental and location-specific issues, overloading, and operational factors. Eventually, they can lose serviceability and may cause public safety issues. The United States has received a "C-" rating for its infrastructure based on an American Society of Civil Engineers (ASCE) report [1]. The federal and state governments have proposed plans to rebuild or rehabilitate the infrastructures. While executing these plans, it is critical to transform our infrastructures into next-generation intelligent civil infrastructure with resilience and sustainability in preparation for facing rapid climate changes and increased natural hazards. Introducing emerging technologies such as advanced materials and sensing technology into infrastructure systems is a promising approach to achieving this objective. Advanced materials with better mechanical performance and durability can significantly enhance the service life of infrastructure. Sensing technology would allow us to access the in-situ structural conditions and evaluate maintenance needs. However, current advanced sensing technologies for monitoring structural integrity require various instrumentations, such as strain gauges, accelerometers, linear variable differential transformers (LVDT), and thermocouples. Although these sensors can collect reliable data, limitations such as low durability, compatibility issues with materials, constant power supply needs, and high installation costs hinder the widespread applications.

In recent years, intrinsic self-sensing cementitious composites have gained much attention due to their excellent compatibility with concrete and relatively low cost compared to sensor instrumentation approaches for large-area sensing [2]. Self-sensing cementitious composites are a novel class of materials that can generate electricity from mechanical strain and can be applied to infrastructures SHM. Due to the piezoresistive effect, SSC can detect temperature and structural strain changes. SSC also has excellent mechanical performance that can replace conventional concrete or perform as a coating layer to rehabilitate existing structures. These properties make SSC a promising alternative for developing intelligent infrastructure monitoring systems. This research will focus on developing self-sensing cementitious composites with high durability that can be used to monitor the structural integrity of different sections of transportation infrastructure, such as reinforced concrete columns, beams, slabs, and even pavements.

Literature Review

The utilization of conductive material in concrete and mortar augments it with a secondary ability: self-sensing [1]. A wide variety of functional/conductive materials such as carbon nanotubes (CNTs) [2], [3], Carbon Black [3], [4], [5], carbon nanofiber [6], [7], [8] graphite nanoplatelet [9], [10], graphene [11], [12], steel fiber [13], [14], [15], nickel powder [16], [17] and TiO_2 [18], [19] have been used as conductive fillers in the past to promote electrical-resistance-based self-sensing. Resistance-based self-sensing is achieved by dispersing these filler materials in cementitious material, which lowers the inherent resistivity of the composite material. An eclectic network of conductive bridges is formed between the filler particles/fibers, which reply to external load with a change in its resistivity. This phenomenon has been described as the piezoresistive effect, percolation mechanism, and quantum tunneling mechanism ([20], [21], [22]. Thus, stress, strain, cracks, and failure can be identified by measuring the change in resistance or impedance under loading. Based on the origin of these fillers, they can be categorized as metal-based and carbon-based conductive fillers.

Metallic (metal-based conductive) fillers have been used in concrete to enhance mechanical and fracture properties [23]. Furthermore, these conductive fillers can also have other functionalities, such as lowering the resistivity of the composite material [24], [25], [26], [27]. Ding et al. [28] performed cyclic flexural loading on concrete beams with 3.5%, 7%, and 11% (by weight of binder) steel fibers (0.55 mm diameter 35 mm length) showed a gauge factor of 1.78, 1.08, and 1.49, respectively. Moreover, in their study, the simultaneous use of 3.5% steel fiber with 0.2% carbon black demonstrated the greatest gauge factor (4.68). Lee et al. [22] used 6 mm length 0.25 mm diameter steel fiber at 2% to promote electrical conductivity in concrete. They concluded that the composite material with metallic fiber showed a clear piezoresistive response under compressive loading. Demircilioglu et al. [29] studied the electrical performance of dosage steel fiber (0%-0.8% by binder volume) with 13 mm length and 0.25 mm diameter in compression-loaded cubic mortar specimens. The highest gauge factor 126.7 was observed in the mix containing 0.8% steel fiber. However, this was measured in the monotonically loaded specimens, which masks the reversibility of this piezoresistive response to loading. Han et al. [16] investigated the piezoresistive effect in composites containing 3-7 μm-sized nickel at 24% by volume of binder. It is found that an unusually high gauge factor of 1929.5 was calculated in monotonic compression loading. Although the metallic fibers exhibit varying levels of electrical response in cementitious material, their susceptibility to environmental

hazards such as corrosion is the major restriction to their broad usage in structural health monitoring [30].

Some carbon-based conductive fillers have been the subject of great interest due to their impressive electrical and thermal capabilities and outstanding mechanical properties [31]. Carbon black is a paracrystalline lump of carbon that exhibits above average electroconductivity, which is essential for its usage as the functional filler in self-sensing concrete. Monteiro et al. studied the effects of carbon black on the electrical resistivity of concrete, where they concluded that 7% carbon black was necessary to reach the percolation threshold (e.g., increasing the conductive filler after point resulted in a minimal increase in gauge factor, or even reduced it) [32]. In another study, they used carbon black at 6.5% and achieved a gauge factor of 40-60 depending on the temperature, with which electrical sensitivity was inversely related [33]. Although carbon black is an economical option for attaining self-sensing concrete, its shortcomings, such as the high percolation threshold, weak resistance to tension and low ductility [34], and increase in porosity [4] in cementitious materials, withhold its broader usage. Carbon nanotubes (CNTs) and carbon nanofibers (CNFs) consist of wrapped graphene sheets [31], [35]. They are considered 1D because of their extremely high aspect ratios (100-2500) [36], [37]. When used with cementitious materials, CNTs and CNFs create electrically conductive webs at the nanoscale, the resistivity of which is sensitive to stress and strain ([38]). Moreover, strengthening the concrete and mortar mixes with the addition of such material, especially CNT, brought by its exceptionally high strength (~40 GPa) and Young's modulus (1 TPa), has become commonplace in the literature [39]. It is reported that using 1% CNF instead of 2% carbon fiber (CF) leads to equivalent or even improved self-sensing ability [40]. For CNT, however, the correlation threshold is reached well below 1%. Konsta-Gdoutos et al. [41], Danoglidis et al. [42], and Luo et al. [43] disclosed that the optimal CNT dosage in cementitious material for the purpose of piezoresistivity was 0.1%, 0.1%, and 0.2%, respectively. In the case of 1-dimensional carbon nanomaterials, their proneness to agglomeration [44] and high price [45] are the bottlenecks for their wide-range utilization. Graphene, graphene nanoplatelets (GNPs), and graphene oxide (GO) are monolayers of graphite, where carbon atoms are aligned uniformly to create a flat two-dimensional surface [46]. These 2D carbon lattices can have a surface area of 2600 m^2/g and an aspect ratio of ~6000; such exceptional geometric qualities cause high elastic modulus, mechanical strength, and electrical conductivity [47]. GO is the functionalized variant of graphene, where oxygen-containing functional groups such as hydroxyl and carbonyl are attached to the graphene lattice. These groups allow a better dispersion of graphene oxide in water [48]. Comparable to CNTs, these fillers also display extraordinary mechanical

properties, which induce enhancements to the electrical [46], mechanical [49], and durability [48] properties of the concrete. For GNPs, Sun et al. [50] report that the percolation threshold was reached at 2 vol%; more interestingly, they discussed the existence of a second percolation at 9 vol%. According to another study [51], the percolation threshold of GNPs was believed to fall between 0.1 and 0.5 wt%. However, in the case of GO, research on its piezoresistive on the cementitious materials was lacking. More research on the contribution of GO to the self-sensing of concrete can bridge this gap in the literature.

Carbon fiber (CF), also known as milled carbon fiber or carbon short fiber, is a fitting candidate for promoting self-sensing in cementitious composites due to its high electrical conductivity, resistance against corrosion, and mechanical properties [45]. Prior studies [31], [52], [53], [54] on the usage of CF as a conductive filler in cementitious composites reveal that the optimal piezoresistivity was captured in the range of 0.5-3%. This, of course, significantly depends on the size, shape, purity, electrical, and other physical characteristics of CF in use. It was previously observed that similar to the dosage of CF, its aspect ratio also affects the resistivity of concrete and, ultimately, its gauge factor [55]. At a constant loading rate, a CF dosage of 0.5wt% and an average fiber diameter of 7.2 μm, increasing the average fiber length from 6 mm to 12 mm increased the gauge factor by 74% to 227%. Zhang et al. [56] report that the percolation threshold at 0.125 vol% was achieved when CF with a 7 μm diameter and a 6 mm length was used in alkali-activated materials. Ma et al. [57], report that the optimal dosage of CF for self-sensitivity was 0.7 vol%. They also investigated the effect of CF on mechanical properties such as compression strength, split tensile strength, and flexural strength. They found that adding 0.5 vol% to 0.9 vol% caused an upward trend in all of these metrics. For large-scale applications in transportation infrastructure, carbon fiber is an economical choice as a conductive filler in developing self-sensing concrete, demonstrating great piezoresistivity at relatively low concentrations.

Since the effect of CF on the piezoresistive and mechanical properties was discovered to be desirable, its long-term impact on the performance of concrete against environmental hazards became the point of discussion [58]. Zhang et al. [58], compared the carbonation depth at 3, 7, 14, and 28 days of the reference concrete with that of carbon fiber-reinforced concrete; increasing the dosage of CF from 0.5% to 1% resulted in a decrease in the depth of 12% to 22%. It was hypothesized that the CF blocked the channels between the pores of concrete, which impeded the permeation of CO^{-3}. Safiuddin et al. [59] studied the influence of 1%-4% CF on the water absorption of cementitious mortar. It was reported that the water absorption dropped at 1%-3% CF, whereas 4% led to a sharp increase in water absorption,

which is attributed to the formation of excessive air voids caused by poor workability and compaction. However, research on the different durability properties of CF-strengthened concrete is limited. The resistance of CF-reinforced concrete against electrical conduction in a corrosive environment requires further investigation.

Objective

This research aimed to develop self-sensing cementitious composites that can be coated on, embedded in, or used as a substitute for conventional concrete in critical structural members of transportation infrastructure to monitor and evaluate their condition autonomously. Furthermore, this study evaluated and enhanced the durability of the proposed materials to improve sustainability for transportation infrastructure applications.

Scope

The scope of this project was to develop self-sensing cementitious materials that are durable for transportation infrastructure implementation. To achieve the objective of the project, comprehensive laboratory tests, including mechanical, electrical, and durability tests, were conducted.

Methodology

Materials

Type I, II Portland Cement manufactured by Holcim per ASTM C150 [60] was used in this study, the chemical composition of which is presented in Table 1. For fine aggregate, an all-purpose sand that meets the ASTM C33 [61] specifications was used. The milled CF with a commercial name of PX35 was procured from Zoltek. The size distribution of CF and OPC is presented in Figure 1. GO was obtained as a 1% solution from Graphenea; for further dilution, water was added and sonicated. The GO had an average particle size of 2-4 μm and the CF had an average particle diameter of 7.2 μm and a length of 120 μm. Particle Size Distribution (PSD) analysis for the cement and CNT was conducted using the Anton Paar Litesizer 500 particle size analyzer. X-ray fluorescence (XRF) analysis was performed through a PANalytical Epsilon 3XLE X-ray Fluorescence Spectroscopy.

Figure 1. Particle size distribution of OPC and CF

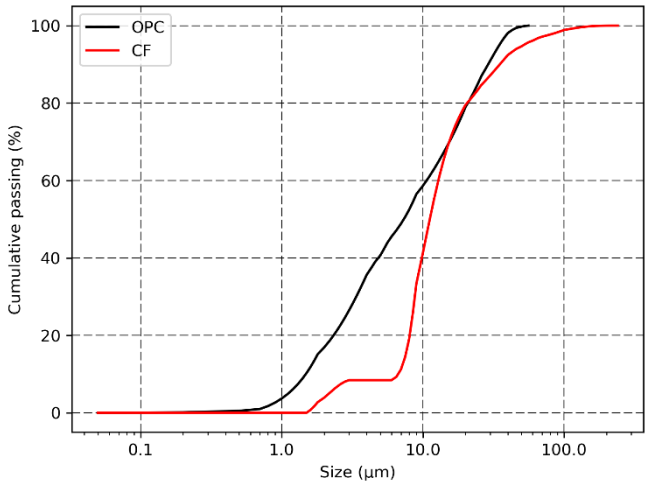

Table 1. Elemental Composition of Graphene Oxide and Carbon Fiber

	Carbon (%)	Oxygen (%)	Hydrogen (%)	Sulfur (%)
Graphene Oxide	49-56	41-50	1-2	2-3
Carbon Fiber	95	-	-	-

Mix Design and Mixing Procedure

After careful deliberation of an effective dosage and type of conductive filler mixed with the cementitious composite, 5 mortar mix designs were considered in this study. Control mix (C) didn't include CF or GO, while 0.1 wt%, 0.5 wt% and 1 wt% CF were added to the CF01, CF05, and CF10 mixtures, respectively. To evaluate the effectiveness of GO as a conductive filler, only 0.1 wt% was incorporated into the cementitious system. The ratios of OPC, sand, and water were kept constant for the mixtures (Table 2.). The conductive filler was added as a solution to the dry material in order to allow for better dispersion. To prevent the agglomeration of CF particles, a bath sonicator with a frequency of 20 kHz was used for 30 minutes. ASTM C305 [62] was followed for the mixing of the mortars, the steps of which are outlined below:

1. Dry mix the OPC and Sand at low speed for 30 seconds
2. Pour in the solution slowly over 30 seconds
3. Mix all ingredients for 30 seconds at medium speed
4. Perform the final mix for 60 seconds at medium speed

After steps 1 and 3, briefly check the material for clumps and scrape the bottom and sides of the bowl.

Table 2. Mix design of cementitious mortar.

	OPC	Sand	Water	Filler Type	Filler Dosage
C	1	1.5	0.45	-	-
CO1	1	1.5	0.45	Carbon fiber	0.001
C05	1	1.5	0.45	Carbon fiber	0.005
C10	1	1.5	0.45	Carbon fiber	0.01
GO-01	1	1.5	0.45	Graphene oxide	0.001

Once the mixing was completed, the mortar was poured into molds that contained 3 spaces for 2" cubes. Before placing material inside the molds, oil was applied to the bottom and

sides to ensure hydrated mortar would not stick to the molds. At the halfway point and end of filling the spaces, the mold was tamped down ten times on each side, and the top layer was made smooth by finishing with a trowel. For the specimens intended for self-sensing, 4 steel strips half an inch in width were embedded. To ensure equal spacing between the strips and the edges, a flat frame with four evenly spaced slots was placed on top of each of the molds after they were filled with the mixture. Finally, the molds were wrapped in stretch wrap to avoid moisture loss. After 24 hours of curing in the molds, the specimens were taken out of their molds and cured in the lab conditions at a temperature of 22 C and a RH of 65%.

Experimental

Compressive testing

The compressive strength of hardened mortar 2x2x2 inch cubes were measured on the 3rd, 7th, and 28th days. For each strength measurement, triplicates were cast. The compressive strength test was conducted per ASTM C109 [63]. The test was performed using a *Gilson AC-325MR* compression machine, where the loading rate applied was 50 psi/s and the preload was 200 lbf. The piezoresistive measurement of monotonically loaded mortar specimens was recorded under similar loading conditions described above.

Flexural testing

ASTM C78 was followed in the testing of the flexural strength of composite prisms that incorporated self-sensing mortar [64]. A 0.2” layer of control mix or one of the test mixes was poured and smoothened on the 28-day concrete substrate. For the application of the layer, the rough surface of the concrete substrate was used. To increase the bonding of the layer and the substrate, no surface coating was used other than wetting. The length, height, and width of the composite prism corresponded to 15.7”, 4”, and 2.2” (this includes the mortar layer). A 4-point bending test was chosen for the flexural test, where all the supports were equidistant (Figure 2.). The modulus of rupture was calculated using the following equation:

$$R = \frac{PL}{bd^2} \quad (1)$$

Where: R, P, L, b, and d, are the modulus of rupture psi, maximum applied load in lbf, the span length in inches, the width of the prism, and the depth of the prism in inches, respectively. The flexural strength setup is presented below:

Figure 2. a) flexural specimen, b) 4-point bending setup for flexure.

(a)

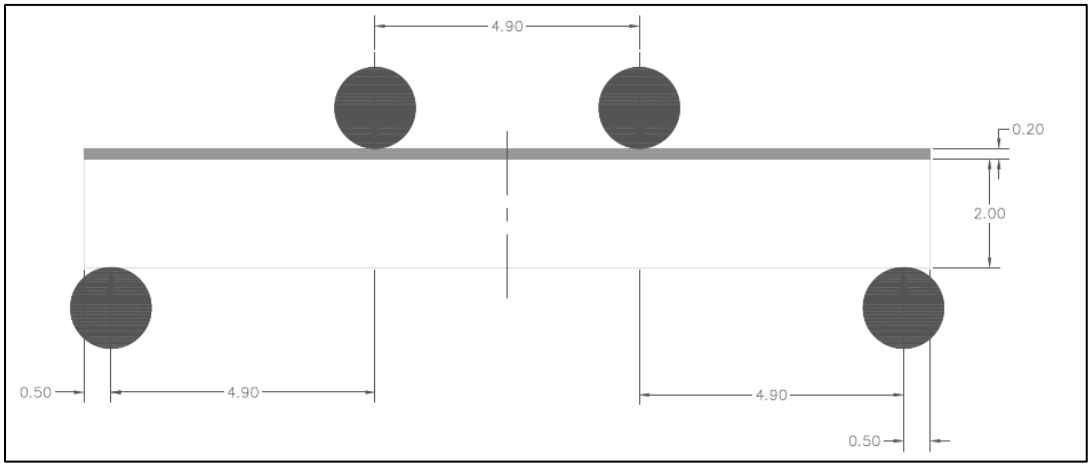

(b)

Electrical resistance

The electrical resistance of the control and test mixture was measured on the 2x2x2-inch cubic specimens. A digital multimeter was used to measure the resistance between the inner two electrodes, with a 0.4” distance embedded in the cube.

Electrical impedance measurement

It is generally recommended that 10%-20% of the ultimate strength of cementitious material should be the upper threshold of stress applied in the cyclic loading. In this investigation, we selected 100 and 1000 psi as the upper and lower limit of loading, respectively. The loading and unloading rate was 35 psi, with a preload of 100 psi. Ten cycles of loading and unloading were applied on each specimen with an upper and lower dwell time of 5 seconds. Due to the limitations of the load-controlled compression machine used in this study, there were some variations in the upper and lower limits of each cycle. Moreover, impedance was measured under monotonic loading until failure.

Figure 3. a) 4-probe cubic specimen b) piezoresistivity testing

(a) (b)

Due to its accuracy, the 4-probe method was used to measure the electrical impedance (Figure 3). The outer electrodes were used to supply the alternative current, and the inner electrodes were used to measure the impedance. A galvanostat with the model number *PGSTAT204* was used to record the electrical impedance. The frequency and current were kept constant at 5 kHz and 10 mA, respectively. Equation (2) and Equation (3) for calculating the impedance and fractional change in resistivity are given below:

$$Z = \frac{V}{I} \quad (2)$$

$$FCR = \frac{Z_i - Z_0}{Z_0} \quad (3)$$

Electrical impedance (Z) is obtained by dividing the voltage (V) by the current (I). FCR is a unitless value obtained from the initial impedance (Z_0) and the impedance at a given load (Z_i). Equation (4), used for deriving the gauge factor (GF), is given below.

$$GF = \frac{FCR}{\varepsilon} \quad (4)$$

Chloride penetration testing

Rapid Chloride Permeability Test (RCPT) was carried out—per ASTM C1202 [65]—on mortar specimens with the same mix design as mentioned previously. Images captured from the cutting, desiccating, and measuring process are illustrated in Figure 4. After following the same mix method used earlier per ASTM C305, mortar specimens were casted into 8” tall cylinder molds with 4” diameters. Similar to the cubic specimens, the bottom and sides of the mold were covered with oil. The mixes were then poured into the molds, while being tamped at 1/3, 2/3, and the final height. Again, after the tamping at the final height, the specimen was given a smooth finish with a trowel. stretch wrap was used to cover the mold, like in the case of the cube molds, until 24 hours, when the specimens were taken out of the molds to continue curing for 27 more days in a water-filled curing container at room temperature.

Once the curing process was completed, the specimen was cut into 2” thick disks using a wet masonry saw. Both faces of the disks were cut by the saw as to ensure each face would be as smooth as possible (neither the top nor bottom of the original cylinder could be used as a face for one of the disks). The new disks were then allowed to air-dry for 24 hours before applying epoxy around the side of the disks. Ten grams of a two-part epoxy were applied around the side of the disks to isolate the walls of the specimen from water and air during the later steps of RCPT. The specimens were left at room temperature for another 24 hours to allow the epoxy to completely dry. To begin the desiccation process, 3 disk specimens were then placed inside a desiccator bought from. The desiccator was connected to a vacuum pump and a separatory funnel through the tubing. The separatory funnel had to be placed at a higher level so water could flow by gravity. However, the water pump and

the desiccator were placed at the same level. For 3 hours, the pump operated at a pressure of 50 mmHg to create a vacuum inside the desiccator and suck out all air from the desiccator and the specimen. During these 3 hours, the connection to the separatory funnel was sealed closed to prevent water from flowing to either the desiccator or the pump. After the three hours were completed, de-aerated water from the separatory funnel flowed into the desiccator to fill the voids that were previously filled with air. The specimens remained submerged underwater in the desiccator for an additional 1 hour while the pump remained active at 50 mmHg of pressure.

Then, the disks were placed inside RCPT Cells purchased from *Giatech*. The specimen had rubber rings placed around both of its faces, allowing it to be placed firmly inside the cells. Each cell had a permeable stainless-steel plate that was in contact with the specimen. One side of the cell is filled with a NaCl solution to make the plate an anode, and the other cell is filled with a NaOH solution, so the plate functions as a cathode, as per ASTM C1202. The ingredients for the two solutions are detailed in Table 3.

Table 3. NaOH and NaCl solutions

Solution	**NaOH (gr)**	**NaCl (gr)**	**Water (gr)**
Anode	14.4	-	1200
Cathode	-	36	1164

Once the specimens were placed inside the cell, per specimen, a power supply of DC 60 volts was connected, and a multimeter was attached parallelly. Electrical resistance and current were measured every 30 minutes, starting from 0 minutes up to 360 minutes. From these current values, the total charge in coulombs could be calculated using Equation (5).

$$Q = 900(I_0 + 2I_{30} + 2I_{60} + 2I_{90} + 2I_{120} \ldots + 2I_{300} + 2I_{330} + 2l_{360}) \quad (5)$$

Q: total current flowing through in Coulombs

I: Current reading in Amperes

Figure 4. a) using masonry saw for cutting the mortar specimen, b) applying epoxy to the sides, c) desiccation, d) taking the measurement of current

(a)

(b)

(c)

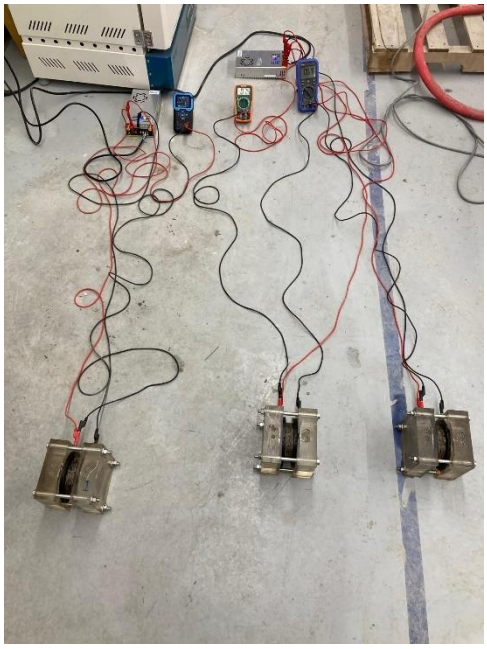

(d)

Half-cell potential corrosion testing

Half-cell testing was conducted in accordance with ASTM C876 [66] to determine the corrosion of activity reinforcing steel embedded into mortar specimens. Mixes C, CF01, CF05, and CF10 were cast into 6” cubic molds. Similar to the previous specimens, the mold had grease applied to all sides before the mixtures were poured inside. The mixes were also tamped at 1/3, 2/3, and the final height to ensure the material was condensed and to minimize large voids. However, this testing involved embedding a singular #3 rebar centered and 2” away from one face of the specimen. The casting and curing of cubic

specimens are shown in Figure 5. A metal wiring was used to keep the rebar in a fixed position. The specimens were allowed to cure for 24 hours in the mold. Once they were demolded, the specimens were placed in a large container, filled with a 10% NaCl solution for five days and then left at room temperature condition for two more days to simulate the harsh coastal environment or cross river bridge in Louisiana. This cycle was repeated four times. At the end of the last cycle, voltage measurements were taken. A copper-copper Sulfate reference electrode was placed at various spots on the face of the specimen, and the rebar was 2” from there. A wetted sponge was used as an electrical junction device to provide an electrical resistance liquid bridge between the mortar and the reference electrode. A multimeter was connected to the reference electrode and to the rebar to measure the potential difference between the metal in the reference electrode and the piece of rebar. If the voltage value is greater than -0.20 V, then no corrosion is most likely occurring in the rebar. Conversely, if the value is less than -0.35 V, corrosion is most likely occurring in the rebar, per ASTM C876 [66].

Figure 5. a) casting of specimen b) curing in saline water

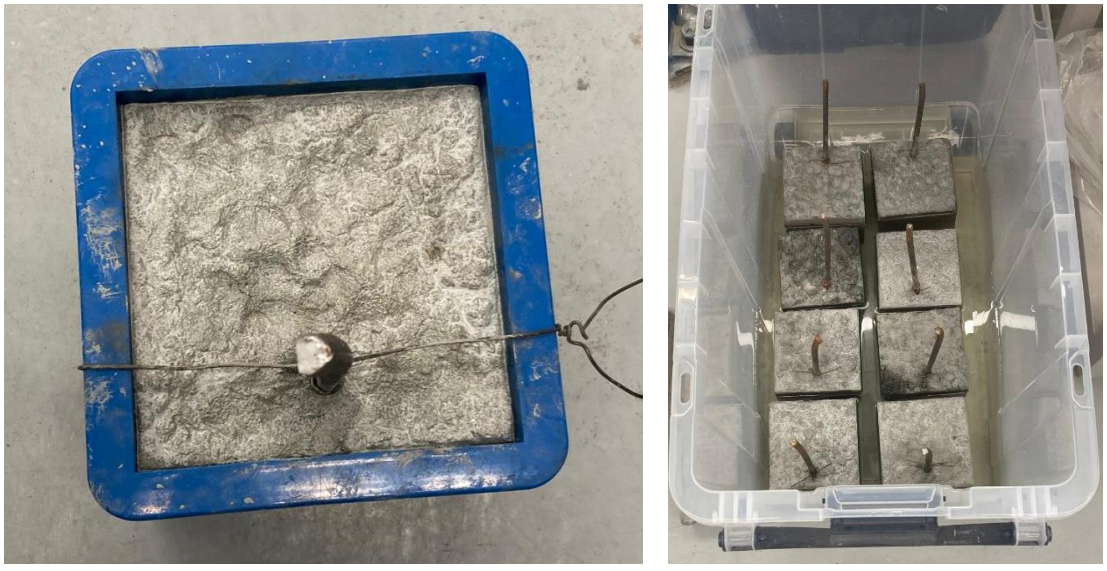

(a) (b)

Discussion & Results

Compressive and Flexural Strength

The compressive strength of different SCC mixes and their development from 1 day to 28 days are presented in Figure 6. below. Control and the test mixtures achieved a strength of more than 6000 psi on the 28th day. The increase in the strength, as expected from the cementitious materials, between 1st and 3rd day was drastic as opposed to the increase between 7 and 28 days. At an early age, the highest compressive strength was observed in the control mix (C). This might be due to the fast hydration rate caused by the availability of water in abundance around the cement particles. However, for 3, 7, and 28 days, the highest compressive strength was recorded for CF05 (0.5% carbon fiber) samples. The ultimate compressive strength for CF05 on the 28th day was 8183 psi. It is possible that the presence of fine carbon fibers with high mechanical properties might have acted as a filler, thus creating a denser microstructure. It is evident that the gap between the strength of control and CF-containing mixes widened as the curing duration increased. The gradual and steady supply of water might have germinated a higher degree of hydration. It is worth noting that a slight decrease in compressive strength was seen when the dosage of CF was increased from 0.5% to 1%. Even though preventing the agglomeration of conductive fillers in cementitious mortar mix via an ultra sonicator was pursued, as the concentration of high-aspect-ratio fine fibers increases, the effort increased for homogenously dispersing them. Therefore, the total volume and/or average size of the pores and faults in the hardened mortar leading to the formation of points of concentrated stress that decrease the strength is speculated to have increased because of the higher amount of CF. The use of GO, on the other hand, even in a lower dosage (0.1%), resulted in lower strength compared to C, especially in the early-age. A 53% drop in 1-day strength was seen when 0.1% GO was introduced to the cementitious mixture. This diminution reduced to a 5% decrease on the 28th day. It can be concluded that the increase in the percentage of CF is relevant to the increase in compressive strength until 1%.

Flexural strength of composite SCC samples is presented in Figure 7. All of the specimens demonstrated a strength of approximately or above 600 psi. The highest strength of 766 psi was seen in the CF01. The effect of carbon fiber on the flexural is not statistically

significant. Since the test mix and reference mix were applied on the top surface of the concrete, the tensile stress was acting on the bottom substrate. Thus, failure is initiated in the substrate.

Figure 6. Compressive strength development

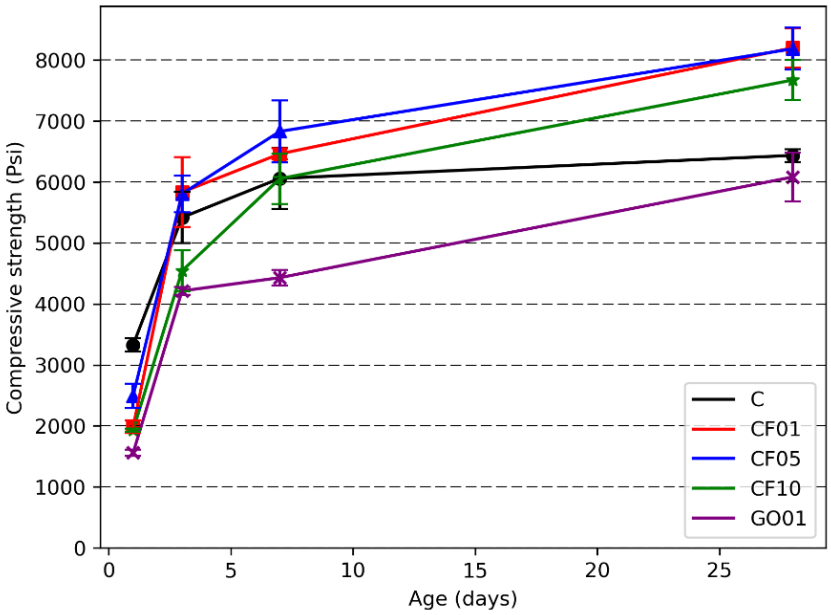

Table 4. Compressive strength on 1, 3, 7, and 28th days

Mixture	1 (psi)	3-day (psi)	7-day (psi)	28-day (psi)
C	3328.7	5417.5	6058.5	6435.5
CF01	1988	5833	6460.5	8199.7
CF05	2494	5805.3	6828.5	8183.7
CF10	1930	4543	6054	7671.3
GO-01	1559	4213.5	4430.3	6081.55

Figure 7. 7th-day flexural strength

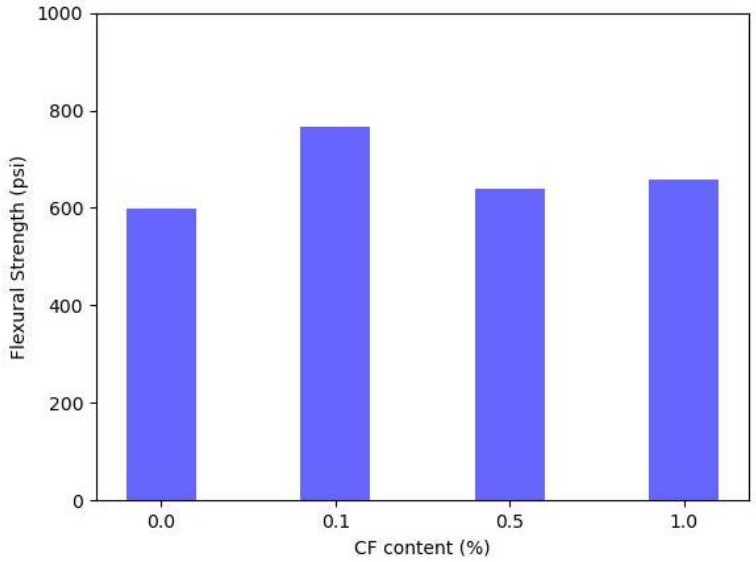

Table 5. flexural strength

Mixture	Flexural Strength (psi)
C	597.67
CF01	766.34
CF05	639.83
CF10	657.68
GO-01	678.37

Piezoresistive self-sensing

Cyclic Loading

The fractional change in resistivity (FCR) is derived from the impedance measured under the cyclic loading of the cubic specimens. The trend of FCR compared to the applied load is presented in Figure 8. No observable correlation between the lines representing FCR and load is seen, meaning the reference mixture doesn't possess measurable piezoresistive properties. As the dosage of conductive filler was increased, the FCR increasingly followed the loading profile more closely. The piezoresistivity was stronger in the GO-containing mixture compared to CF-based composites. Even 0.1% GO seems more potent in impacting the FCR than 1% of carbon fiber. Gauge factor (GF) is the calculable representation of the potency of various conductive fillers in dispensing the piezoresistive effect to cementitious materials. The GF is shown in the Table 6 The highest GF of 75.62 was achieved in CF10 (1% carbon fiber) sample. As the amount of CF was increased, GF displayed a similar progression. The effect of GO-01 has a GF of 39.37 is, which comparable to the GF of CF05, 40.61. This proves that a lower dosage of GO compared to CF, 1/5 in this case, endows similar self-sensing efficacy to the mortar. One possibility for the occurrence of this disparity is the difference in the size which entails a significant divergence in aspect ratio and specific surface area of these to fillers. The CF used in this study had an average diameter and length of 7.2 and 120 μm, the aspect ratio of which is approximated to 16.7. More than 95% of GO, on the other hand, is comprised of monolayer content. The thickness of single layer of GO is estimated to be 0.7 nm [67]. The diameter of the GO sheet on average is 3000 nm. Therefore, the percolation network formed by the filler particles is more refined and effective in lowering the resistivity.

Figure 8. Fractional change in resistivity vs. cyclic loading

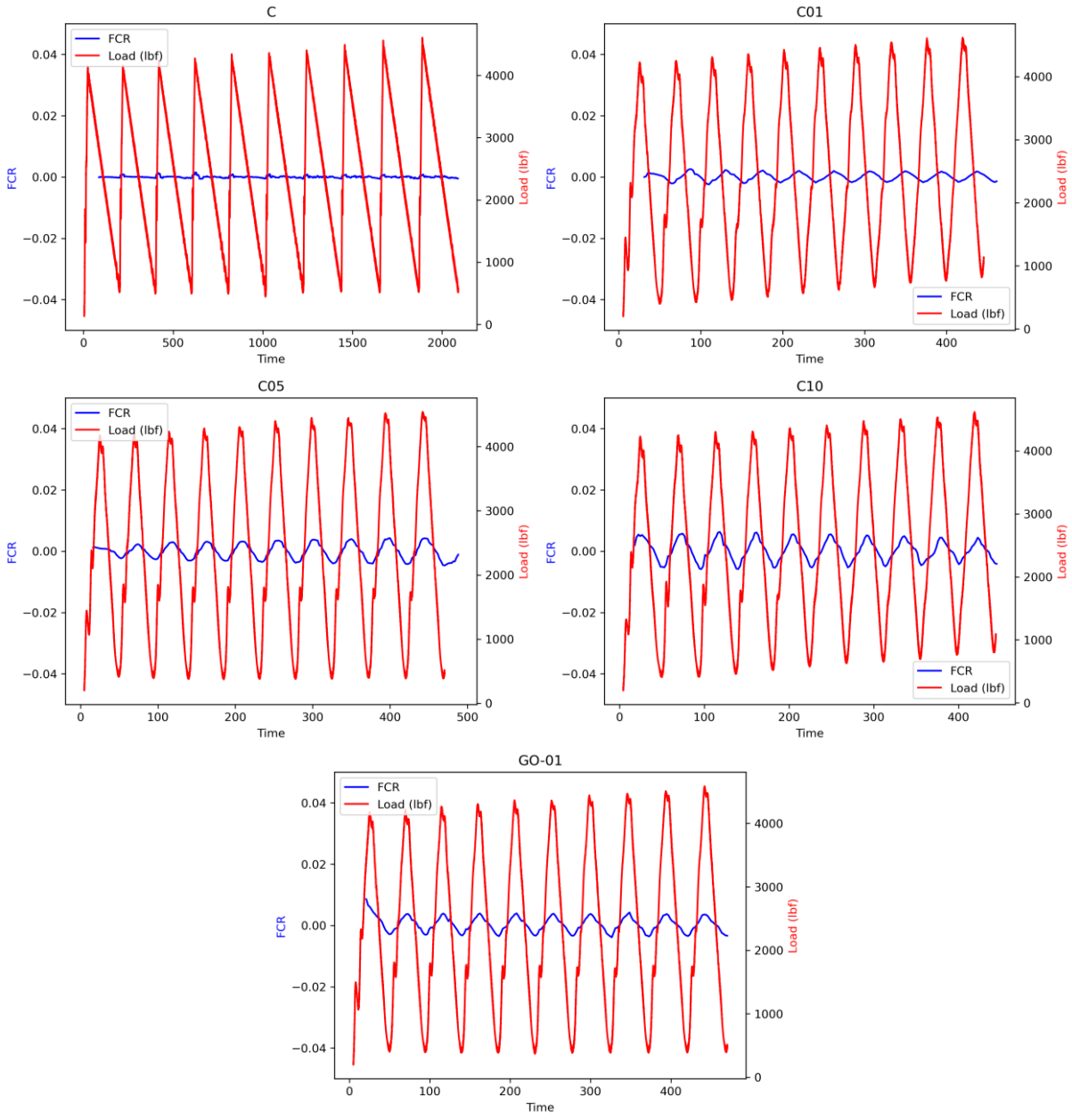

To better understand the electrical properties of the cement composites, their electrical resistance was also measured, which is provided in Table 6. The electrical resistance amongst the different mixtures ranged between 189 and 144 KΩ. As the percentage of CF was increased, electrical resistance dropped. The highest resistance was observed in the

control mixture, whereas the lowest was seen in the CF10. The impact of GO on resistance was similar to its effect on GF; the resistance of GO-01 was similar to that of CF05.

Table 6. Gauge factor and electrical resistance of mortar mixtures

Mixture	Gauge Factor	Electrical resistance (KΩ)
C	-	189
CF01	22.83	180
CF05	40.61	178
CF10	75.62	144
GO-01	39.37	177

Monotonic Loading

The change in impedance was measured under monotonic loading until the specimen reached failure. FCR and load in pounds (lbs) versus time for all the mixtures plotted in Figure 9. The self-sensing observations under monotonic loading reveal that FCR doesn't always follow the loading pattern. However, a sharp increase in FCR under approximately 3000 lbs of load and close to failure was seen in the piezoresistive mixtures. The latter peak was not significant in the control sample due to the absence of any conductive fibers.

Figure 9. Fractional change in resistivity versus monotonic loading

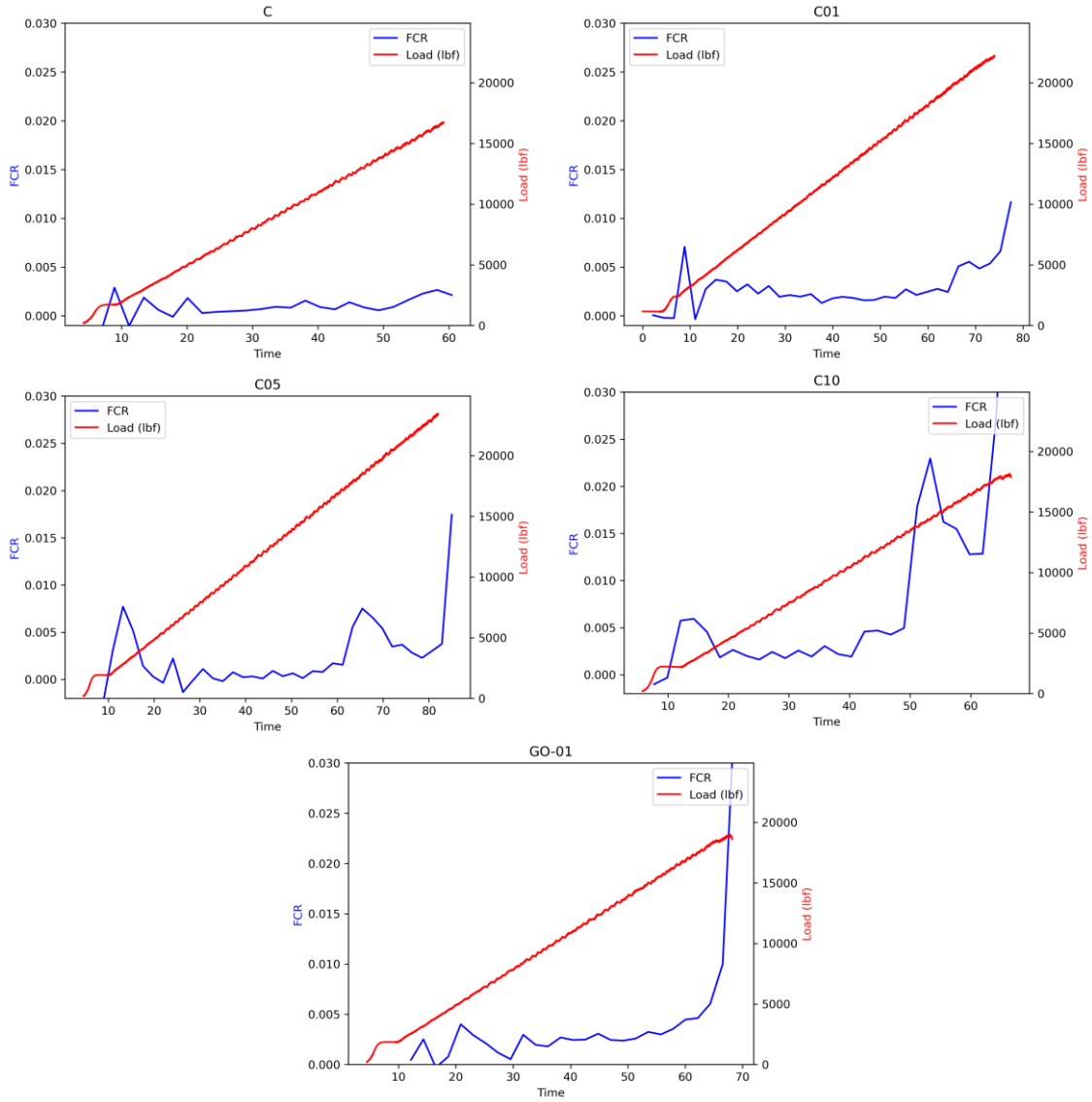

Durability

Based on the results of self-sensing and mechanical tests, only the sample with carbon fiber were designed for durability tests due to the economic consideration.

Rapid Chloride Penetration

Rapid chloride penetration test (RCPT) results are presented as the total amount of charge passed in Coulombs in Figure 10. ASTM C1202 indicates the following qualitative chloride ion penetrabilities: high, moderate, low, very low, and negligible. Amongst the different mixtures investigated in this study, only the control mix penetrability of above 4000 coulombs, which places it in the highly penetrable category. CF hindered the passing of the charge in the concrete; CF01 had a total amount of charge (Q) of 3227.4 C. The lowest Q of 2644.2 was seen in the CF10. This improvement in the impenetrability of cementitious composite is theorized to be due to the pore refining capability of micro-scale functional fillers [68]. Granted CF is an electrically conductive carbon-based filler, and it might lead to an increase in the total porosity of cementitious materials, however, it is beyond doubt its dispersion causes a decrease in the volume of large capillary pores. Hence, the permeability and penetrability are reduced.

Figure 10. Chloride permeability of cementitious mixes

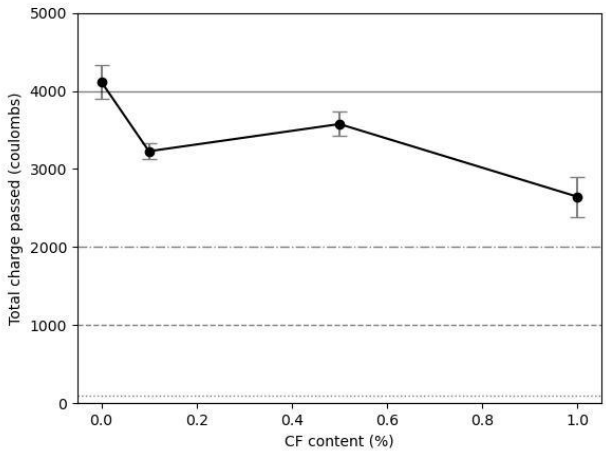

Table 7. Total charge passed vs. the CF dosage

CF content	0%	0.1%	0.5%	1%
Total charge passed (C)	4116.1	3227.4	3575.7	2644.2

Half-cell potential corrosion testing

According to Bertolini et al. [69], the passivity potential of reinforced concrete depends on the environment. The potential of passivity ranges between +50 and -200 mV in reinforced concrete components subjected to atmospheric conditions. This potential is decreased when the reinforced concrete is exposed to corrosive environments with a high CO^{-3} or Cl^{-} concentration. It is reported that chloride-induced pitting causes a more intense negative passivity potential of -400 to -700 mV.

The potential of passivity for the mixtures prepared in this study is shown in Figure 11. Since the mortar specimens were subjected to a corrosive environment (10% concentration of saline water), the initial voltage was much lower. To account for this difference in curing condition, the passivity potential was normalized. The effect of carbon-based functional fillers was not statistically significant. The voltage ranged from 156-206 -mV. As the percentage of CF increased, so did the magnitude of the potential. This is due to the higher diffusion rate of oxygen molecules. The only mixture that is at risk of corrosion in normal conditions is CF10, which is placed in the “an increasing probability of corrosion” zone. Contradictory to RCPT, the excessive addition of CF increased the risk of corrosion slightly. However, all the mixtures except CF10 remained in the 90% probability of no corrosion zone.

Figure 11. Probability of corrosion

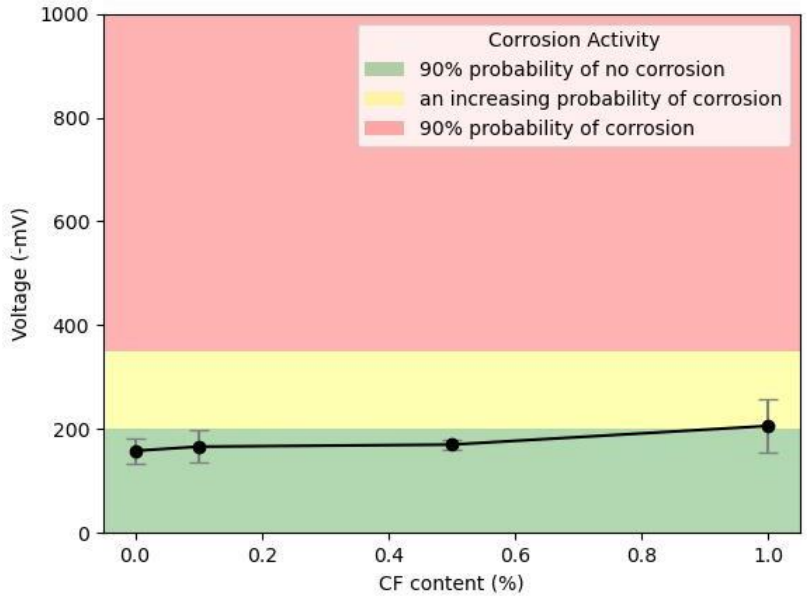

Table 8. The negative voltage in mV vs. different dosages of CF

CF content (%)	0	0.1	0.5	1
Voltage (-mV)	158	166	170	206

Conclusions

The following conclusion on the durable self-sensing composites were drawn from this study:

- Carbon fiber (CF) is an appropriate conductive filler for the enhancement of the self-sensing abilities of cementitious composite due to its high gauge factor, low price, and easy dispersion in the mix.
- Graphene oxide (GO) is effective in forming a percolation network for the purposes of conducting electricity in the cementitious materials, even in much smaller quantities compared to other fillers.
- Compressive strength is affected by the inclusion of carbon-based fillers. CF is effective in improving the long-term strength development, whereas in the short term, it had a deleterious effect on the compressive strength. GO lowered the strength in all of the tested ages.
- Chloride penetration was hindered by utilizing CF significantly. The high risk of corrosion was lowered to moderate by including 1% of CF in the mixture.

Recommendations

It is recommended that in the future investigations, the other durability tests such as water-permeability test, carbonation test, and shrinkage test should be taken into consideration to have comprehensive understanding of long-term durability of self-sensing concrete.

Acronyms, Abbreviations, and Symbols

Term	Description
AASHTO	American Association of State Highway and Transportation Officials
CF	Carbon
FHWA	Federal Highway Administration
FCR	Fractional change in resistivity
GF	Gauge factor
GO	Graphene oxide
HCP	Half-cell potential
in.	inch(es)
LADOTD	Louisiana Department of Transportation and Development
LTRC	Louisiana Transportation Research Center
lbs.	pounds
RCPT	Rapid chloride penetration test
m	meter(s)

References

[1] D. D. L. Chung, “A critical review of electrical-resistance-based self-sensing in conductive cement-based materials,” *Carbon*, vol. 203. Elsevier Ltd, pp. 311–325, Jan. 25, 2023. doi: 10.1016/j.carbon.2022.11.076.

[2] T. Yin, J. Xu, Y. Wang, and L. Liu, “Increasing self-sensing capability of carbon nanotubes cement-based materials by simultaneous addition of Ni nanofibers with low content,” *Constr Build Mater*, vol. 254, p. 119306, 2020, doi: 10.1016/j.conbuildmat.2020.119306.

[3] S. Wen and D. D. L. Chung, “Partial replacement of carbon fiber by carbon black in multifunctional cement-matrix composites,” *Carbon N Y*, vol. 45, no. 3, pp. 505–513, 2007, doi: 10.1016/j.carbon.2006.10.024.

[4] M. G. Pârvan, G. Voicu, and A. I. Bădănoiu, “Study of hydration and hardening processes of self-sensing cement-based materials with carbon black content,” *J Therm Anal Calorim*, vol. 139, no. 2, pp. 807–815, 2020, doi: 10.1007/s10973-019-08535-8.

[5] H. Deng and H. Li, “Assessment of self-sensing capability of Carbon Black Engineered Cementitious Composites,” *Constr Build Mater*, vol. 173, pp. 1–9, 2018, doi: 10.1016/j.conbuildmat.2018.04.031.

[6] O. Galao, F. J. Baeza, E. Zornoza, and P. Garcés, “Strain and damage sensing properties on multifunctional cement composites with CNF admixture,” *Cem Concr Compos*, vol. 46, pp. 90–98, 2014, doi: 10.1016/j.cemconcomp.2013.11.009.

[7] O. Galao, F. J. Baeza, E. Zornoza, and P. Garcés, “Carbon nanofiber cement sensors to detect strain and damage of concrete specimens under compression,” *Nanomaterials*, vol. 7, no. 12, 2017, doi: 10.3390/nano7120413.

[8] M. S. Konsta-Gdoutos and C. A. Aza, “Self sensing carbon nanotube (CNT) and nanofiber (CNF) cementitious composites for real time damage assessment in smart structures,” *Cem Concr Compos*, vol. 53, pp. 162–169, 2014, doi: 10.1016/j.cemconcomp.2014.07.003.

[9] H. Du, S. T. Quek, and S. D. Pang, “Smart multifunctional cement mortar containing graphite nanoplatelet,” *Sensors and Smart Structures Technologies for Civil, Mechanical, and Aerospace Systems 2013*, vol. 8692, no. November, p. 869238, 2013, doi: 10.1117/12.2009005.

[10] W. Dong, W. Li, X. Zhu, D. Sheng, and S. P. Shah, “Multifunctional cementitious composites with integrated self-sensing and hydrophobic capacities toward smart structural health monitoring,” *Cem Concr Compos*, vol. 118, no. January, p. 103962, 2021, doi: 10.1016/j.cemconcomp.2021.103962.

[11] D. Y. Yoo, I. You, and S. J. Lee, “Electrical properties of cement-based composites with carbon nanotubes, graphene, and graphite nanofibers,” *Sensors (Switzerland)*, vol. 17, no. 5, 2017, doi: 10.3390/s17051064.

[12] S. Dong, L. Li, A. Ashour, X. Dong, and B. Han, “Self-assembled 0D/2D nano carbon materials engineered smart and multifunctional cement-based composites,” *Constr Build Mater*, vol. 272, p. 121632, 2021, doi: 10.1016/j.conbuildmat.2020.121632.

[13] S. H. Lee, S. Kim, and D. Y. Yoo, “Hybrid effects of steel fiber and carbon nanotube on self-sensing capability of ultra-high-performance concrete,” *Constr Build Mater*, vol. 185, pp. 530–544, 2018, doi: 10.1016/j.conbuildmat.2018.07.071.

[14] S. Wen and D. D. L. Chung, “A comparative study of steel- and carbon-fibre cement as piezoresistive strain sensors,” *Advances in Cement Research*, vol. 15, no. 3, pp. 119–128, 2003, doi: 10.1680/adcr.15.3.119.36621.

[15] D. Y. Yoo, S. Kim, and S. H. Lee, “Self-sensing capability of ultra-high-performance concrete containing steel fibers and carbon nanotubes under tension,” *Sens Actuators A Phys*, vol. 276, pp. 125–136, 2018, doi: 10.1016/j.sna.2018.04.009.

[16] B. G. Han, B. Z. Han, and J. P. Ou, “Experimental study on use of nickel powder-filled Portland cement-based composite for fabrication of piezoresistive sensors with high sensitivity,” *Sens Actuators A Phys*, vol. 149, no. 1, pp. 51–55, 2009, doi: 10.1016/j.sna.2008.10.001.

[17] B. G. Han, B. Z. Han, and X. Yu, “Effects of the content level and particle size of nickel powder on the piezoresistivity of cement-based composites/sensors,” *Smart Mater Struct*, vol. 19, no. 6, 2010, doi: 10.1088/0964-1726/19/6/065012.

[18] L. Zhang, L. Li, Y. Wang, X. Yu, and B. Han, “Multifunctional cement-based materials modified with electrostatic self-assembled CNT/TiO2 composite filler,” *Constr Build Mater*, vol. 238, p. 117787, 2020, doi: 10.1016/j.conbuildmat.2019.117787.

[19] S. Laflamme and F. Ubertini, “Back-to-Basics : Self-Sensing Materials for Nondestructive Evaluation,” *Self-Sensing Materials for Nondestructive Evaluation, Materials Evaluation*, pp. 1–12, 2019.

[20] M. Abedi, R. Fangueiro, and A. Gomes Correia, “A review of intrinsic self-sensing cementitious composites and prospects for their application in transport infrastructures,” *Constr Build Mater*, vol. 310, no. April, 2021, doi: 10.1016/j.conbuildmat.2021.125139.

[21] D. A. Triana-Camacho, J. H. Quintero-Orozco, E. Mejía-Ospino, G. Castillo-López, and E. García-Macías, “Piezoelectric composite cements: Towards the development of self-powered and self-diagnostic materials,” *Cem Concr Compos*, vol. 139, 2023, doi: 10.1016/j.cemconcomp.2023.105063.

[22] S. Y. Lee, H. V. Le, and D. J. Kim, “Self-stress sensing smart concrete containing fine steel slag aggregates and steel fibers under high compressive stress,” *Constr Build Mater*, vol. 220, pp. 149–160, 2019, doi: 10.1016/j.conbuildmat.2019.05.197.

[23] J. Thomas and A. Ramaswamy, “Mechanical Properties of Steel Fiber-Reinforced Concrete”, doi: 10.1061/ASCE0899-1561200719:5385.

[24] D. D. L. Chung, “Strain sensors based on the electrical resistance change accompanying the reversible pull-out of conducting short fibers in a less conducting matrix,” *Smart Mater Struct*, vol. 4, no. 1, pp. 59–61, 1995, doi: 10.1088/0964-1726/4/1/009.

[25] M. T. Kazemi, H. Golsorkhtabar, M. H. A. Beygi, and M. Gholamitabar, “Fracture properties of steel fiber reinforced high strength concrete using work of fracture

and size effect methods," *Constr Build Mater*, vol. 142, pp. 482–489, 2017, doi: 10.1016/j.conbuildmat.2017.03.089.

[26] J. Han, M. Zhao, J. Chen, and X. Lan, "Effects of steel fiber length and coarse aggregate maximum size on mechanical properties of steel fiber reinforced concrete," *Constr Build Mater*, vol. 209, pp. 577–591, 2019, doi: 10.1016/j.conbuildmat.2019.03.086.

[27] T. Ferdiansyah, A. Turatsinze, and J. P. Balayssac, "Design and characterization of self-sensing steel fiber reinforced concrete," *MATEC Web of Conferences*, vol. 199, 2018, doi: 10.1051/matecconf/201819911008.

[28] Y. Ding, G. Liu, A. Hussain, F. Pacheco-Torgal, and Y. Zhang, "Effect of steel fiber and carbon black on the self-sensing ability of concrete cracks under bending," *Constr Build Mater*, vol. 207, pp. 630–639, 2019, doi: 10.1016/j.conbuildmat.2019.02.160.

[29] E. Demircilioglu, E. Teomete, and O. E. Ozbulut, "Strain sensitivity of steel-fiber-reinforced industrial smart concrete," *J Intell Mater Syst Struct*, vol. 31, no. 1, pp. 127–136, 2020, doi: 10.1177/1045389X19888722.

[30] A. Beglarigale and H. Yazıcı, "Electrochemical corrosion monitoring of steel fiber embedded in cement based composites," *Cem Concr Compos*, vol. 83, pp. 427–446, Oct. 2017, doi: 10.1016/j.cemconcomp.2017.08.004.

[31] J. Han, J. Pan, J. Cai, and X. Li, "A review on carbon-based self-sensing cementitious composites," *Constr Build Mater*, vol. 265, Dec. 2020, doi: 10.1016/j.conbuildmat.2020.120764.

[32] A. O. Monteiro, P. B. Cachim, and P. M. F. J. Costa, "Self-sensing piezoresistive cement composite loaded with carbon black particles," *Cem Concr Compos*, vol. 81, pp. 59–65, 2017, doi: 10.1016/j.cemconcomp.2017.04.009.

[33] A. O. Monteiro, A. Loredo, P. M. F. J. Costa, M. Oeser, and P. B. Cachim, "A pressure-sensitive carbon black cement composite for traffic monitoring," *Constr Build Mater*, vol. 154, pp. 1079–1086, 2017, doi: 10.1016/j.conbuildmat.2017.08.053.

[34] X. Li and M. Li, “Multifunctional self-sensing and ductile cementitious materials,” *Cem Concr Res*, vol. 123, 2019, doi: 10.1016/j.cemconres.2019.03.008.

[35] M. H. Al-Saleh and U. Sundararaj, “Review of the mechanical properties of carbon nanofiber/polymer composites,” *Composites Part A: Applied Science and Manufacturing*, vol. 42, no. 12. pp. 2126–2142, Dec. 2011. doi: 10.1016/j.compositesa.2011.08.005.

[36] T. Wang, J. Xu, B. Meng, and G. Peng, “Experimental study on the effect of carbon nanofiber content on the durability of concrete,” *Constr Build Mater*, vol. 250, Jul. 2020, doi: 10.1016/j.conbuildmat.2020.118891.

[37] B. Han, K. Zhang, T. Burnham, E. Kwon, and X. Yu, “Integration and road tests of a self-sensing CNT concrete pavement system for traffic detection,” *Smart Mater Struct*, vol. 22, no. 1, Jan. 2013, doi: 10.1088/0964-1726/22/1/015020.

[38] L. Li *et al.*, “Carbon nanotube (CNT) reinforced cementitious composites for structural self-sensing purpose: A review,” *Construction and Building Materials*, vol. 392. Elsevier Ltd, Aug. 15, 2023. doi: 10.1016/j.conbuildmat.2023.131384.

[39] M.-F. Yu, B. S. Files, S. Arepalli, and R. S. Ruoff, “Tensile Loading of Ropes of Single Wall Carbon Nanotubes and their Mechanical Properties,” 2000.

[40] F. J. Baeza, O. Galao, E. Zornoza, and P. Garcés, “Multifunctional cement composites strain and damage sensors applied on reinforced concrete (RC) structural elements,” *Materials*, vol. 6, no. 3, pp. 841–855, 2013, doi: 10.3390/ma6030841.

[41] M. S. Konsta-Gdoutos and C. A. Aza, “Self sensing carbon nanotube (CNT) and nanofiber (CNF) cementitious composites for real time damage assessment in smart structures,” *Cem Concr Compos*, vol. 53, pp. 162–169, 2014, doi: 10.1016/j.cemconcomp.2014.07.003.

[42] P. A. Danoglidis, M. S. Konsta-Gdoutos, E. E. Gdoutos, and S. P. Shah, “Strength, energy absorption capability and self-sensing properties of multifunctional carbon nanotube reinforced mortars,” *Constr Build Mater*, vol. 120, pp. 265–274, 2016, doi: 10.1016/j.conbuildmat.2016.05.049.

[43] L. Jianlin *et al.*, “Piezoresistive properties of cement composites reinforced by functionalized carbon nanotubes using photo-assisted Fenton,” *Smart Mater Struct*, vol. 26, no. 3, Feb. 2017, doi: 10.1088/1361-665X/aa559d.

[44] D. D. L. Chung, “A critical review of electrical-resistance-based self-sensing in conductive cement-based materials,” *Carbon*, vol. 203. Elsevier Ltd, pp. 311–325, Jan. 25, 2023. doi: 10.1016/j.carbon.2022.11.076.

[45] M. Abedi, R. Fangueiro, and A. Gomes Correia, “A review of intrinsic self-sensing cementitious composites and prospects for their application in transport infrastructures,” *Constr Build Mater*, vol. 310, no. April, 2021, doi: 10.1016/j.conbuildmat.2021.125139.

[46] O. Sevim, Z. Jiang, and O. E. Ozbulut, “Effects of graphene nanoplatelets type on self-sensing properties of cement mortar composites,” *Constr Build Mater*, vol. 359, Dec. 2022, doi: 10.1016/j.conbuildmat.2022.129488.

[47] W. Li, F. Qu, W. Dong, G. Mishra, and S. P. Shah, “A comprehensive review on self-sensing graphene/cementitious composites: A pathway toward next-generation smart concrete,” *Construction and Building Materials*, vol. 331. Elsevier Ltd, May 09, 2022. doi: 10.1016/j.conbuildmat.2022.127284.

[48] H. Chu, Y. Zhang, F. Wang, T. Feng, L. Wang, and D. Wang, “Effect of graphene oxide on mechanical properties and durability of ultra-high-performance concrete prepared from recycled sand,” *Nanomaterials*, vol. 10, no. 9, pp. 1–17, Sep. 2020, doi: 10.3390/nano10091718.

[49] M. Devasena, J. Karthikeyan, and M. E. Student, “INVESTIGATION ON STRENGTH PROPERTIES OF GRAPHENE OXIDE CONCRETE,” *International Journal of Engineering Science Invention Research & Development*, vol. I, p. 307, 2015, [Online]. Available: www.ijesird.com

[50] S. Sun *et al.*, “Nano graphite platelets-enabled piezoresistive cementitious composites for structural health monitoring,” *Constr Build Mater*, vol. 136, pp. 314–328, Apr. 2017, doi: 10.1016/j.conbuildmat.2017.01.006.

[51] J. Tao, X. Wang, Z. Wang, and Q. Zeng, “Graphene nanoplatelets as an effective additive to tune the microstructures and piezoresistive properties of cement-based

composites," *Constr Build Mater*, vol. 209, pp. 665–678, Jun. 2019, doi: 10.1016/j.conbuildmat.2019.03.173.

[52] G. Yıldırım, O. Öztürk, A. Al-Dahawi, A. Afşın Ulu, and M. Şahmaran, "Self-sensing capability of Engineered Cementitious Composites: Effects of aging and loading conditions," *Constr Build Mater*, vol. 231, Jan. 2020, doi: 10.1016/j.conbuildmat.2019.117132.

[53] J. Wen, Z. Xia, and F. Choy, "Damage detection of carbon fiber reinforced polymer composites via electrical resistance measurement," *Compos B Eng*, vol. 42, no. 1, pp. 77–86, Jan. 2011, doi: 10.1016/j.compositesb.2010.08.005.

[54] Y. Rew, A. Baranikumar, A. V. Tamashausky, S. El-Tawil, and P. Park, "Electrical and mechanical properties of asphaltic composites containing carbon based fillers," *Constr Build Mater*, vol. 135, pp. 394–404, Mar. 2017, doi: 10.1016/j.conbuildmat.2016.12.221.

[55] F. J. Baeza, O. Galao, E. Zornoza, and P. Garcés, "Effect of aspect ratio on strain sensing capacity of carbon fiber reinforced cement composites," *Mater Des*, vol. 51, pp. 1085–1094, 2013, doi: 10.1016/j.matdes.2013.05.010.

[56] W. Zhang *et al.*, "Effects of recycled carbon fibers on mechanical and piezoresistive properties and environmental impact in alkali-activated cementitious materials," *J Clean Prod*, vol. 450, Apr. 2024, doi: 10.1016/j.jclepro.2024.141902.

[57] L. Ma, M. Sun, and Y. Zhang, "The Mechanical and Self-Sensing Properties of Carbon Fiber- and Polypropylene Fiber-Reinforced Engineered Cementitious Composites Utilizing Environmentally Friendly Glass Aggregate," *Buildings*, vol. 14, no. 4, p. 938, Mar. 2024, doi: 10.3390/buildings14040938.

[58] J. Zhang, J. Cheng, Y. Dou, and Q. Xin, "Mechanical properties and durability of fiber-reinforced concrete," *Journal of Engineering Science and Technology Review*, vol. 10, no. 5, pp. 68–75, 2017, doi: 10.25103/jestr.105.08.

[59] M. Safiuddin, G. Abdel-Sayed, and N. Hearn, "Absorption and strength properties of short carbon fiber reinforced mortar composite," *Buildings*, vol. 11, no. 7, Jul. 2021, doi: 10.3390/buildings11070300.

[60] “Designation: C 150-07 Standard Specification for Portland Cement 1.” [Online]. Available: www.astm.org

[61] “Designation: C33/C33M − 23 Standard Specification for Concrete Aggregates 1”, doi: 10.1520/C0033_C0033M-23.

[62] ASTM C305, “Standard Practice for Mechanical Mixing of Hydraulic Cement Pastes and Mortars of Plastic Consistency,” *ASTM lnternational*, pp. 1–3, 2011.

[63] ASTM C109, “Standard Test Method for Compressive Strength of Hydraulic Cement Mortars,” *ASTM International*, vol. 04, no. May, pp. 1–6, 1999.

[64] American Society of Testing and Materials, “Standard Test Method for Flexural Strength of Concrete (Using Simple Beam with Third-Point Loading) 1,” *ASTM C78*, 2010, doi: 10.1520/C0078-09.

[65] “Standard Test Method for Electrical Indication of Concrete’s Ability to Resist Chloride Ion Penetration 1”, doi: 10.1520/C1202-22E01.

[66] “Standard Test Method for Corrosion Potentials of Uncoated Reinforcing Steel in Concrete 1.” [Online]. Available: www.astm.org,

[67] J. W. Suk, R. D. Piner, J. An, and R. S. Ruoff, “Mechanical properties of monolayer graphene oxide,” *ACS Nano*, vol. 4, no. 11, pp. 6557–6564, Nov. 2010, doi: 10.1021/nn101781v.

[68] L. Bostanci, “Effect of pore structure properties on strength properties of hybrid silica fume mortars containing randomly distributed carbon fibers,” *Asian Journal of Civil Engineering*, vol. 22, no. 7, pp. 1377–1399, Nov. 2021, doi: 10.1007/s42107-021-00389-6.

[69] L. Bertolini, *Corrosion of steel in concrete : prevention, diagnosis, repair*. Wiley-VCH, 2004.